

The Influence of Transfection Methods on the Molecular Dynamics of the Cell Plasma Membrane



Guo Meihui, Thorsten Wholand, and Saphthaswaran Veerapathiran

Abstract Lipofection is an example of transfection, where foreign nucleic acids are coupled with cationic lipids and delivered into the cell via endocytosis [16]. However, lipofection is a traumatic event for the cells. Due to the lack of elucidation on how lipofection affects cell membrane dynamics and the duration for the cell to recover, this study aims to elucidate the duration of membrane re-organization. To achieve the aims of this study, CHO-K1 are transfected with Glycosylphosphatidylinositol tagged Green Fluorescent Protein (GPI-GFP) and exposed to 488 nm laser light, leading to GFP fluorescent emission (510 nm), which is subsequently recorded on a fast camera. The fluctuations in fluorescence intensity in each pixel are measured by Imaging Fluorescent Correlation Spectroscopy (ImFCS), which correlates the fluctuations in the fluorescent intensity to obtain the diffusion coefficient of GPI-GFP. The results of determining the diffusion coefficient over different length scales (by 21×21 pixel binning) are used in the FCS Diffusion law to produce a diffusion law plot, where the y-intercept values of the plots give insights on the modes of diffusion. This experiment showed that plasma membrane recovery post lipofection is surprisingly robust, with no significant membrane perturbations observed.

Keywords Transfection · Lipofection · Fluorescent microscopy

1 Introduction

Transfection is the process of introducing foreign nucleic acids into eukaryotic cells. It is a fundamental technique for the study of biochemical and physiological processes of cells and has been applied to genetically manipulate mammalian cells to express high levels of selected proteins [15]. Such technology is an important area in health-care as it could enable large-scale production of desired products such as insulin,

G. Meihui (✉)

Hwa Chong Institution, Singapore, Singapore

e-mail: guomeihui50@gmail.com

T. Wholand · S. Veerapathiran

BioImaging Sciences, NUS, Singapore, Singapore

© The Author(s), under exclusive license to Springer Nature Singapore Pte Ltd. 2021

H. Guo et al. (eds.), *IRC-SET 2020*,

https://doi.org/10.1007/978-981-15-9472-4_12

141

interferon, and even viral vaccines [3, 13, 18]. Common transfection methods include electroporation, microinjection, viral transfection and lipofection. All transfection procedures are traumatic events for the cells, as the membrane porosity required for deliverance of foreign genes into the cell inevitably creates micropores that severely disrupts membrane integrity. Previous studies have shown that the cellular responses to such membrane perturbations contributed to the differential expression of the gene of interest, which not only pose difficulty in understanding which effects are the true biological responses to the specific gene, but also negatively impacts the identification and production of desired proteins for clinical use [6–8]. As a result, various studies have been conducted to investigate the effects of transfection on cell membrane. However, there is a lack of elucidation on how lipofection, a process by which foreign nucleic acids are coupled with cationic lipids delivered into the cell via endocytosis and phagocytosis, in particular, affects cell membrane dynamics [16]. Since this process requires extensive interactions between the cationic DNA-lipid complexes and the cell membrane, it is expected that lipofection would cause observable cell membrane perturbations and result in temporary or permanent membrane changes. Therefore, the aim of this study is fill in the gap in our understanding of how lipofection affect cell membrane organization and experimentally elucidate the duration for the cell membrane to recover after lipofection.

To elucidate how lipofection affect cell membrane dynamics, a fundamental understanding of the cell membrane is necessary. The cell plasma membrane is a biological barrier that covers the cell surface, separates the cell from its extracellular environments and ensures proper cellular functioning by regulating cellular interactions between adjacent cells and the extracellular environment. Recent studies have shown that the cell membrane is non-homogenous and highly segregated into compartmentalized microdomains, also known as lipid rafts [14]. Lipid rafts are distinct regions on the cell membrane with a higher concentration of cholesterol, glycosphingolipids, and glycosylphosphatidylinositol (GPI)-anchored proteins. There is now increasing evidence suggesting that lipid rafts are instrumental in regulation of important cellular processes such as cell polarity, protein trafficking, and signal transduction [4, 5]. For example, cell membrane surface receptors such as the epidermal growth factor receptor are known to be involved in cell proliferation, differentiation and survival [1, 10]. In addition, lipid rafts are also known as the modulator of sensitivity of cell signaling during tissue morphogenesis [9]. Studies have also revealed that confinement by lipid rafts allows for the receptors and cofactors to meet at an increased rate and hence speed up cell responses. Together, these reports point to the fact that lipid rafts influence an array of critical biological events and play crucial roles in the plasma membrane organization. Given the significant role of lipid rafts in cell membrane organization, GPI-anchors, which are known to be associated with lipid rafts, are therefore chosen as the marker for cell membrane organization. GPI-anchors and tagged with Green Fluorescent Protein (GPI-GFP) to enable monitoring of GPI-GFP fluorescence and hence localizations of GPI anchors, thereby giving insights on the cell membrane organization post lipofection.

Conventionally, the study of diffusion modes of fluorescent molecules is conducted via Fluorescent Correlation Spectroscopy (FCS), an analytical tool that

performs statistical analysis of fluctuation data to give diffusion coefficients and diffusion times of fluorescent molecules in femtoliter volumes. However, due to interference between neighboring confocal volumes, conventional FCS requires a minimum distance 10–15 confocal diameters between focal volume elements, hence limiting the confocal spots in FCS experiments [17, 19]. To improve on the conventional FCS technique, Total Internal Reflection FCS (TIRF-FCS), which selectively illuminating only a thin layer of the sample that lies in the focal plane of the detection objective and thus reduces interferences between the detection elements, is used in this experiment to obtain more measurements per sample per time interval with less phototoxicity. Nevertheless, TIRF-FCS is still constrained by the Abbe diffraction limit, which states that regardless of how an optical instrument is manufactured, its resolving power will always be diffraction-limited to scales of 200–360 nm for optical wavelengths [2, 11, 12]. Lipid rafts, typically around 20–100 nm are well below this fundamental limit of diffraction. Therefore, the diffusion behavior of lipid rafts and the raft-associated proteins cannot be observed directly. To resolve this challenge, FCS diffusion law, an analytical technique that plots the diffusion time (τ_d) against the observation area (A_{eff}), was used in conjunction of TIRF-FCS to deduce the mode of diffusion of GPI-GFP. Extrapolation of the diffusion law plot gives the y-intercepts, which provide insights on the diffusion mode of fluorescent molecules. For freely diffusing molecules, the y intercept is zero as τ_d is directly proportional to A_{eff} . For raft-associated molecules, y intercept is positive as the diffusing molecules are obstructed and slowed down by the presence of lipid rafts. For hop diffusion due to meshwork confinement, y intercept is negative (Fig. 1).

Continuous monitoring of the mode of diffusion of GPI-GFP post lipofection provides answers to the state of cell membrane reorganization, and the duration for the cell membrane to recover after lipofection.

1.1 Methods and Results

A. Cell culturing

CHO-K1 cells were cultivated in Dulbecco's Modified Eagle Medium (DMEM; Invitrogen, Singapore), a liquid medium with high concentration of amino acids and vitamins, to achieve sustained cell growth. Fetal Bovine Serum (FBS), which has high content of embryonic growth factors, was added at 10% concentration to promote cell growth. 1% Penicillin-Streptomycin (PS) was added to control gram-positive and gram-negative bacterial contamination and the cells were maintained at 37 °C and 5% v/v CO₂ to create optimum growth conditions. When the cells covered 90% surface area of a T75 flask (90% confluent), the DMEM was removed, 3 ml of Phosphate Buffered Saline (PBS) was added to rinse the flask, and 2 ml of trypsin was subsequently added to detach the cells from the flask. 10 ml of DMEM was added 2 min after trypsinization to neutralize the effects of trypsin. The detached cells were then seeded on 35 mm glass-covered dishes (No. 1.0 cover glass 0.13–0.16 mm,

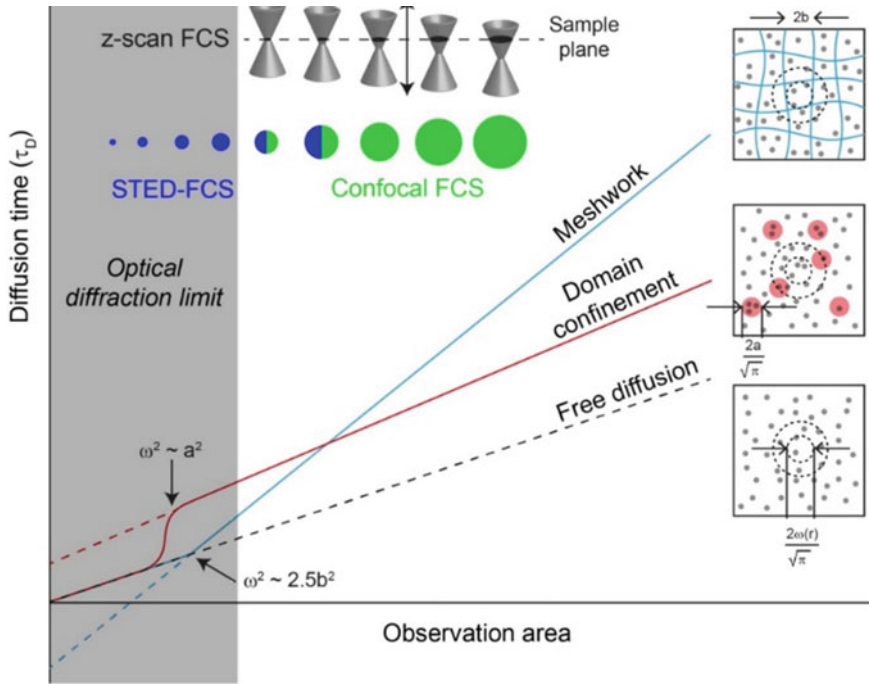


Fig. 1 FCS diffusion law plots for various diffusion modes in the membrane: free diffusion (black dotted line), hindered diffusion in domain confinement (red line) and hop diffusion in meshwork compartmentalization (light blue line) are illustrated. Reprinted from X. Ng et al. (2015)

Matek Corporation, US) with fresh DMEM, 10% FBS and 1%PS and incubated at 37 °C and 5% v/v CO₂ for 48 h to achieve 90% confluence.

B. Lipofection procedure

In a sterile Eppendorf tube, 6 microliters of Lipofectamine 3000™ reagent (L3000; Invitrogen, Singapore) was diluted in 125 microliters of Opti-MEM Reduced Serum Media (Opti-MEM, Invitrogen, Singapore). In another sterile Eppendorf tube, 2 microliters of GFP-GPI plasmid (Anovasia Pte Ltd, Singapore) and 4 microliters of P3000™ reagent (Invitrogen, Singapore) was diluted in 125 microliters of Opti-MEM. The diluted GFP-GPI plasmid was added to the diluted L3000 reagent and the resulting complex was incubated for 10 min at room temperature. After incubation, the complex was added to the 90% confluent CHO-K1 cells for transfection. The transfected cells were incubated at 37 °C and 5% v/v CO₂ and fluorescent expression was monitored every 30 min post transfection up to 10 h, at which fluorescent expression could be observed under a 4X light microscope. The transfected cells were then washed with Hank's Balanced Salt Solution (HBSS; Invitrogen, Singapore) and maintained in Phenol red-free DMEM and 10% FBS at 37 °C and 5% v/v CO₂.

C. TIRF FCS instrumentation

A Total Internal Reflection Fluorescence (TIRF) microscope (IX83, Olympus, Singapore) was equipped with an Electron Multiplying Charge Coupled Device (EMCCD) camera (Andor iXon2 X-9388, 128×128 pixels; Andor Technology, US), a 488 nm excitation laser (Olympus Cell Lasers 488; Olympus, Singapore), and a oil-immersion objective (UApoN100x, Olympus, Singapore). The principal attribute of a TIRF microscope is the utilization of evanescent wave to excite the fluorescent molecules, as opposed to excitation via direct laser light. The energy of the evanescent wave is concentrated in the vicinity of the glass-specimen interface, and therefore the penetration depth into the specimen is limited to a few hundred nanometers. This spatially limited excitation range allows for exclusive excitation of fluorescent particles in a small observation area located close to the interface and significantly increases signal-to-noise ratio, making the TIRF microscope ideal for imaging of fluorescent-tagged dynamic reactions in the cell membrane. The transfected cell cultures were maintained at 37 °C and 5% v/v CO₂ by an incubator with an objective heater (Live Cell Instruments, CU-109, Chambridge, Seoul, Korea) and a CO₂ gas chamber (Live Cell Instruments, FC-05, Chambridge, Seoul, Korea). The 488 nm excitation beam was focused on the sample by a tilting mirror and a dichromic mirror. The Olympus Xcellence software was used to achieve total internal reflection via automatic calibration of the incident angle of the laser beam. The signal reflected by the objective was filtered by an emission filter (ZET405/488561/647 m, Chroma Technology, USA) and directed to the EMCCD camera.

D. Data collection

A 21×21 pixels ($5 \times 5 \mu\text{m}^2$) region of interest on the cell was captured by 30 000 frames at 3 ms exposure. The Kinetic image acquisition mode was utilized with a readout rate of 10 MHz, a vertical shift speed of 45 μs and an electron multiplier gain level of 300 (in a scale of 6–1000). The recorded image stacks were processed with ImFCS 1491 plugin from ImageJ. Correlation of the intensity fluctuations of each pixel by ImFCS 1491 provides autocorrelation function (ACF) curves according to Eqs. (1)–(2), and subsequently gives a plot of diffusion time against the observation area, from which the diffusion coefficient (D) and the number of particles (N) could be obtained.

$$G(\tau) = \sum_i^{N_d} \alpha_i \left[\frac{\text{erf}(p(\tau)) + \frac{-(p(\tau))^2 - 1}{\sqrt{\pi} p(\tau)}}{\text{erf}(p(0)) + \frac{-(p(0))^2 - 1}{\sqrt{\pi} p(0)}} \right] \left[1 + \left(\frac{F_t}{1 - F_t} \right) \exp\left(-\frac{\tau}{t_f}\right) \right] + G_\infty \quad (1)$$

$$p(\tau) = \frac{a}{\sqrt{4D\tau_o^2}} \quad (2)$$

$$\alpha_i = \frac{B_i^2 \langle N_i \rangle}{(B_i \langle N_i \rangle)^2} \quad (3)$$

In the equations above, $G(\tau)$ represents ACF model as a function of time (τ). The pixel length is denoted by a , and the Gaussian approximation of microscope point spread function, which is the three-dimensional image of a point-like fluorescent molecule under the microscope, is denoted by ω_o . The average number of fluorescent molecules is denoted by $\langle N_i \rangle$ and the brightness of the fluorescent molecules is denoted by B_i . The proportion of fluorescent particles in the triplet state and the duration spent in the triplet state are denoted by F_t and t_f respectively. The convergence value after a long lag time is denoted by G_∞ .

The ImFCS diffusion law is the plot of τ_d against A_{eff} , according to Eqs. (4)–(5)

$$(A_{eff}) = \tau_o + \frac{A_{eff}}{D} \quad (4)$$

$$A_{eff}(\tau) = \frac{a^2}{\frac{\omega_o}{\left[a\sqrt{\pi} \left(e^{-\frac{a^2}{\omega_o^2} - 1} \right) + \text{erf} \left(\frac{a}{\omega_o} \right) \right]^2}} \quad (5)$$

2 Results

A TIFR-FCS microscope is used to record the intensity fluctuations of the GPI-GFP fluorescence, which are subsequently autocorrelated by software ImFCS 1491 to give a graph of $G(\tau)$ against τ , also known as an ACF curve (Fig. 2). From the ACF curve, the diffusion coefficient (D) and the number of particles (N) could be obtained. D is then feed into the diffusion law to produce a graph of τ_o against observation area (Fig. 3), from which the duration for the cell membrane to recover to its native state could be deduced.

Fig. 2 Representative experimental auto correlation function (ACF) curve for CHO-K1 cells transfected with GPI-GFP

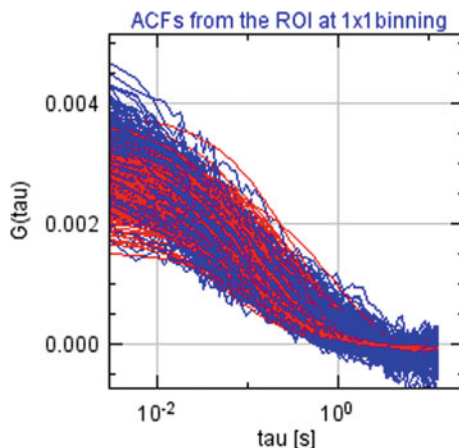
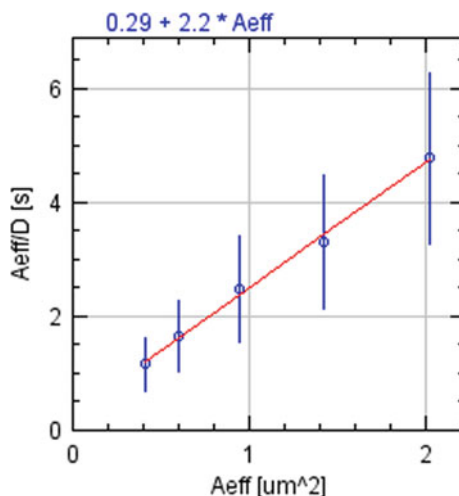


Fig. 3 Representative diffusion law plot for CHO-K1 cells transfected with GPI-GFP with a τ_o of 0.29



Interestingly, D shows no significant fluctuations as time progresses (Fig. 4). D remains relatively constant at $0.34 \mu\text{m}^2/\text{s}$, with a D value of $0.40 \pm 0.07 \mu\text{m}^2/\text{s}$ at the 10th h and a D value of $0.31 \pm 0.02 \mu\text{m}^2/\text{s}$ at the end of the 24th h. Similarly, average τ_o show no significant fluctuations (Fig. 5). τ_o remains relatively constant at 0.67 s , with a τ_o value of $0.63 \pm 0.26 \text{ s}$ at the start of 10th h to $0.78 \pm 0.21 \text{ s}$ at end of the 24th h. Since all τ_o values are positive, it can be inferred that GPI-GFP molecules are undergoing domain confined diffusion.

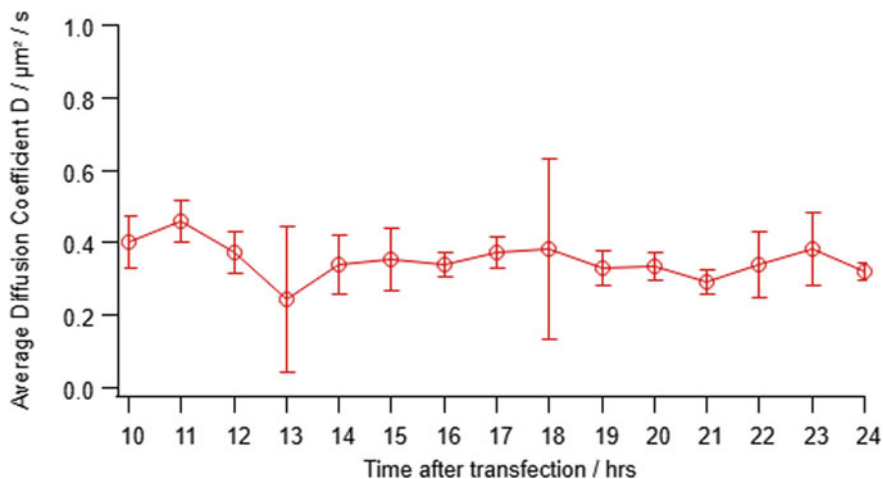


Fig. 4 Graph of average diffusion coefficient (D) against time after transfection

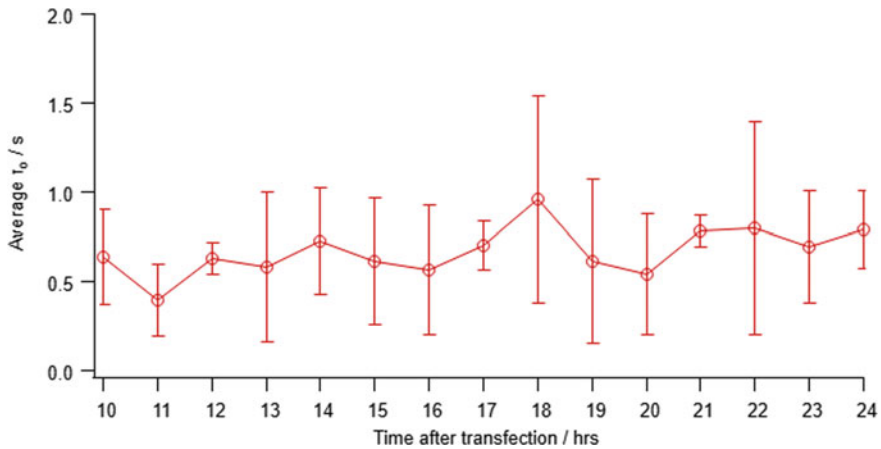


Fig. 5 Graph of average τ_0 against time after transfection

3 Discussion

The stability of D and τ_0 is surprising as it is expected that the lipofection procedure would cause observable cell membrane perturbations. The relative stability of D and τ_0 suggest that the cell membrane recovered significantly by the 10th h post transfection. This is in stark contrast to previous electroporation experiments done by other members of our lab, which showed that both D and τ_0 values stabilize only after the 13th h. This suggests that lipofection is not only a less invasive transfection method as compared to electroporation, but also do not significantly disturb cell membrane organizations. Another possible explanation for the apparent stability of D and τ_0 values could be that by the time fluorescent expressions are observable, the membrane perturbations caused by lipofection have attenuated significantly. Following cellular internalization of GFP-GPI via endocytosis, the GFP-GPI would appear in the endosomes and later in the nucleus. It is still unclear how the GFP-GPI are released from the endosomes and traverse the nuclear membrane. After reaching the nucleus, the integration of GFP-GPI into the DNA of host cells and the eventual fluorescent expressions requires yet more time. These series of events ultimately result in a observable time lag between actual membrane perturbations immediately after lipofection and the first expression of fluorescence after 10 h. Therefore, the relative stability of membrane organizations post lipofection could be explained by the fact that the any actual perturbations of cell membrane immediately post lipofection are not captured due to the inherent limitation of the lipofection technique used in this experiment.

4 Conclusion

The results suggest that the duration for the cells to recover after lipofection is less than 10 h. This observation would be useful for future researchers seeking to perform various kinds of transfection on cells to study expression of desired proteins. Nevertheless, more question regarding the membrane perturbances caused by lipofection immediately after lipofection procedures are generated. Further elucidation on the duration of recovery of cell membrane post lipofection would fill in the gap in our understanding of the effects of lipofection of cell membrane organization, hence helping researchers performing the procedure to better understand the differential expressions of gene of interest post lipofection, which ultimately results in better identification and production of desired proteins for clinical use. Further research could be performed with probes targeting other regions, such as the non-raft regions and the actin cytoskeleton meshwork, to investigate if similar results would be obtained. Moreover, temporal study of other transfection methods such as sonoporation, microinjection and viral transduction could be conducted to investigate how other transfection methods affect membrane dynamics.

Acknowledgements I would like to thank Professor Thorsten Wohland for providing mentorship and support throughout my project. I would also like to express my gratitude to my mentor Sathaswaran Veerapathiran, who has kindly assisted me throughout the project, particularly in the learning of how to use equipment stated in the methodology, growing of CHO-K1 samples, and guiding the analysis of the experiments.

References

1. Hoeller D, Volarevic S, and Dikic I. (2005), "Compartmentalization of growth factor receptor signalling," *Current Opinion in Cell Biology*, 17, 107–111. <https://doi.org/10.1016/j.ceb.2005.01.001>
2. Baddeley D, Jayasinghe D, Lam L, Rossberger S, Cannell M. B, and Soeller C. (2009). "Optical single-channel resolution imaging of the ryanodine receptor distribution in rat cardiac myocytes," *Proceedings of the Natural Academy of Sciences. U.S.A.* 106, 22275–22280. <https://doi.org/10.1073/pnas.0908971106>
3. Roca-Cusachs P, Gauthier N. C, Del Rio A, and Sheetz M. P. (2009). "Clustering of alpha (5) beta (1) integrins determines adhesion strength whereas alpha (v) beta (3) and talin enable mechanotransduction," *Proceedings of the Natural Academy of Sciences. U.S.A.* 106, 16245–16250. <https://doi.org/10.1073/pnas.0902818106>
4. Singer S. J., Nicolson L. (1972). "The Fluid Mosaic Model of the Structure of Cell Membranes," *Science*. Feb: Vol. 175, Issue 4023, pp. 720–73. <https://science.sciencemag.org/content/175/4023/720/tab-pdf>
5. Simons K, Ikonen E. (1997). "Functional rafts in cell membranes," *Nature*. 387. 569–72.
6. Simons K, Vaz W L. (2004). *Annual Review of Biophysics and Biomolecular Structure*. 33:269–95.
7. Klaasse E C, Ijzerman A P, and Beukers M W. (2008). Internalization and desensitization of adenosine receptors. *Purinergic Signal*. 4, 21–37. <https://doi.org/10.1007/s11302-007-9086-7>

8. Batada N, Shepp L A, and Siegmund D O. (2004). "Stochastic model of protein–protein interaction: why signaling proteins need to be colocalized," *Proceedings of the National Academy of Sciences. Sci. U.S.A.* 101, 6445–6449. <https://doi.org/10.1073/pnas.0401314101>
9. Catherine S. (2011). "In DNA transfection, efficiency and cytotoxicity are two sides of the same coin," *Biocompare*. <https://www.biocompare.com/Editorial-Articles/41821-In-DNA-Transfection-Efficiency-and-Cytotoxicity-Are-Two-Sides-of-the-Same-Coin/>
10. Prevette L. E, Mullen, D. G, Holl M. (2010). "Polycation-induced cell membrane permeability does not enhance cellular uptake or expression efficiency of delivered DNA," *Molecular pharmaceutics*, 7(3), 870–883. <https://www.ncbi.nlm.nih.gov/pmc/articles/PMC2882516/>
11. Stelzer E. "Beyond the diffraction limit," *Nature* 417, 806–807 (2002) <https://doi.org/10.1038/417806a>
12. Jagadish S, Andreas K, Scott A. R, Thorsten W. (2018). "Quantitative imaging and spectroscopic technologies for microbiology," *FEMS Microbiology Letters*. Volume 365, Issue 9, May, fny075. <https://doi.org/10.1093/femsle/fny075>
13. Sathaswaran V, Thorsten Wohland. (2018). "The imaging FCS law in the presence of multiple diffusive modes," *Methods*. May 1;140–141:140-150.
14. Lingwood D, Kaiser HJ, Levental I, Simons K. (2009) "Lipid rafts as functional heterogeneity in cell membranes," *Biochemical Society Transactions*. Oct;37(Pt 5):955–60.
15. Kusumi A, Sako Y. (1996). "Cell surface organization by the membrane skeleton," *Current Opinion in Cell Biology*. Aug, 8(4), 566–74
16. Kim T K, & Eberwine J H. (2010). "Mammalian cell transfection: the present and the future," *Analytical and bioanalytical chemistry*, 397(8), 3173–3178, <https://www.ncbi.nlm.nih.gov/pmc/articles/PMC2911531/>
17. Linda B Jacobsen, Susan A Calvin, Edward K. Lobenhofer (2018). "Transcriptional effects of transfection: the potential for misinterpretation of gene expression data generated from transiently transfected cells," *Biotechniques*. VOL. 47, NO. 1. <https://doi.org/10.2144/000113132>
18. Griffiths AJF, Miller JH, Suzuki DT. "An Introduction to Genetic Analysis," 7th edition. New York: W. H. Freeman; 2000. Recombinant DNA technology in eukaryotes. <https://www.ncbi.nlm.nih.gov/books/NBK22002/>
19. Elson E L. (2011). "Fluorescence correlation spectroscopy: past, present, future," *Biophysical journal*, 101(12),2855–2870. <https://doi.org/10.1016/j.bpj.2011.11.012>